KSME International Journal, Vol. 11, No. 4, pp. 443~456, 1997

Local Characteristics of Two-Phase Flow Parameters in an Annulus Boiling Channel

Byong-Jo Yun*, Suk-K. Sim*, Su-Hyun Hwang and Goon-Cherl Park****

(*Received July 30, 1996*)

Local two-phase flow parameters were measured to investigate the internal flow structures of steam-water boiling flow in an annulus channel. Two kinds of measuring methods for the local two-phase flow parameters were investigated. A two-conductivity probe was used for local vapor parameters and a Pitot tube for local liquid parameters. Using these probes, the distributions of phasic velocities, interfacial area concentration (IAC) and void fraction are measured in a steam-water boiling flow. In this study, it is observed that the local void fraction is smoothly decayed out from the surface of a heating rod to the channel center in subcooled boiling without any wall void peaking, which were observed in air-water experiments. The distributions of the local IAC and bubble frequency coincide with those of the local void fraction for a given area-averaged void fraction.

Key Words: Steam-Water Boiling Flow, Two-Conductivity Probe, Pitot Tube, Void Fraction, Phasic Velocity, Interfacial Area Concentration, Bubble Frequency

Nomenclature

$a_i(r)$: Local interfacial area concentration (1/m)
D_h : Hydraulic diamater (m)
D_s : Local sauter diameter (m)
j_l : Local liquid superficial velocity (m/sec)
k : Momentum transfer factor of Pitot tube in the single phase flow
L : Channel length (m)
N_{szj} : Number of bubble velocity v_{szj}
N_t : Bubble numbers per second
V_b : Vapor bubble velocity (m/sec)
v_{szj} : Velocity measured by a two-conductivity probe (m/sec)
v_{sz} : Arithmetic mean of v_{szj}
v_L : Local liquid velocity (m/sec)
ΔZ : Probe distance (m)
α : Local void fraction
ρ_g, ρ_l : Phase density for vapor and liquid (kg/m^3)
Δp : Dynamic pressure of the Pitot tube
τ : Time difference between probes (sec)
$\langle\phi\rangle$: Area average of parameter ϕ

* Korea Atomic Energy Reserach Institute, Taejon, 305-600, Korea.
** Departement of Nuclear Engineering Seoul National University, Seoul, 151-742, Korea

1. Introduction

Two-phase flow phenomena have been studied with theoretical and experimental methods for engineering applications in nuclear thermal hydraulics and other related industries. In particular, precise prediction of the phasic behaviors in subchannels under two-phase flow conditions is of great importance to the safety analysis of nuclear power plants and the verification of the thermal-hydraulic design code. The measurements of distributions of the local two-phase flow parameters are needed to get detailed informations on the flow structure of two-phase flow. But the measurements of local phasic parameters in two-phase flow are very difficult since application of currently avaliable instrumentation is limited and the phasic behaviors are so complicated to understand. For a few decades, a considerable amount of works on the measurements of the local two-phase flow parameters have been successfully performed by many investigators since Neal(1963)'s work on the measurement of local void profile in an air-water flow condition. Serizawa(1974) measured the turbulence structure of air-water bubbly flow, Kataoka et. al (1984) measured local IAC in air-water bubbly flow, Welle(1985) measured the local two-phase flow parameters in air-water flow, Sim et. al (1986) measured phase distributions in a complex flow channel. In these experimental works, the flow structure of air-water two-phase flow was figured out and the exact prediction of phase distribution in air-water flow condition was possible.

Most of those works were, however, limited to adiabatic flow conditions like air-water flow and thus more comprehensive understanding on the two-phase flow phenomena are needed to predict the local two-phase flow parameters in boiling channels. Especially, measurements of the distributions of local two-phase flow parameters are essentially necessary because they give us detailed informations on the flow structures of boiling flow.

The present work is an experimental study on the measurements of the local phasic parameters in a steam-water boiling flow. For this, an annulus boiling channel was set up and the measuring techniques for the local phasic parameters were investigated. The instrumentations developed here are a two-conductivity probe method for local vapor parameters and a Pitot tube method for local liquid parameters, both of which are applicable to the steam-water boiling flow condition. By applying these techniques, the distributions of the local void fraction, local phasic velocities, local vapor turbulent fluctuation and the local IAC were measured simultaneously in a steam-water boiling flow. The system pressure and liquid superficial velocity of the test channel are 1 bar and less than 2 m/sec, respectively, and the flow regime considered is limited to the developing region between the subcooled and the bulk boiling.

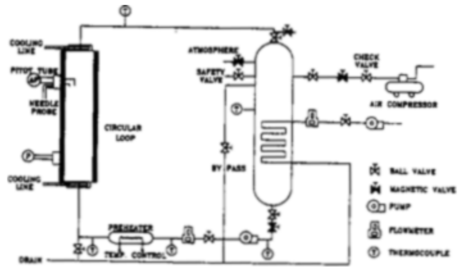

Fig. 1 Schematic diagram of test loop

2. Experimental Facility

The boiling loop is composed of, as shown in Fig. 1, a test channel, a cooler, a pump and a preheater. The test channel is designed to be an annulus type, that is, a circular stainless steel tube of 33 mm I. D. having a heating rod with 16 mm O. D. inside the annulus region. The test channel is 2 m in length and the flow area of the test channel is 6.54cm^2. The maximum heat generation rate of the heating rod is 30kW and the heat generation rate can be controlled by the thyrister chip. The local probes are located 1.6m downstream of the inlet of the test channel (L/D_h= 94). A traversing system to position local probes consists of a ball slide unit and a micro vernier meter with 1/100mm spatial resolution.

3. Measuring Methods

3.1 Local measurement of vapor phase

In this study, the local parameters of vapor phase are measured by the two-conductivity probe method. This method is described below.

3.1.1 Two-conductivity probe method

The two-conductivity probe method is based on the electrical resistance difference between the vapor and the liquid phase. It was developed first by Neal in 1963. And then Serizawa(1974), Herring & Davis(1976), Welle(1983) and Liu (1989) used the two-conductivity probe method in the measurements of local bubble parameters in air-water flow. More recently a multi-sensor probe method to measure the local void fraction and local IAC was developed by Ishii and Revan-

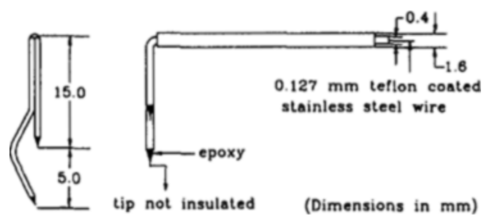

Fig. 2 Schematic diagram of two-conductivity probe

kar (1990).

The two-conductivity probe used in this study is shown in Fig. 2. The distance between two probe tips should be selected properly to measure the bubble velocity with sufficient accuracy. If the probe distance is too long, bubbles which pass the start probe may be scattered without touching the stop probe. Many previous investigators reported that the most suitable distance between tips is about 5mm. However, more attention is needed to the determination of the proper probe distance in the steam-water boiling flow because the bubble is generated or grown on the surface of the heating rod. In the analysis of high-speed photograph, the probe distance of 4 to 5 mm is found to be also proper in this boiling experiments. Measurements of the probe distance are performed with an electron microscope with a spatial resolution of 1/1000mm. The instantaneous measurements of local resistivity changes in the two-phase stream are converted into voltage drops reading by a AC rectifier circuit.

3.1.2 Determination of the cutoff level for phase discrimination

The determination of the proper cutoff level, which is the boundary between the two phases, is very important to get the accurate measurements of void fractions and bubble velocities.

Many previous researchers, such as Neal & Bankoff(1963), Herring & Davis(1976) and Serizawa(1974), used the Schmitt triggering circuit with a preset constant cutoff level for all bubbles. But this preset cutoff level is not always proper because the output signal is varied by probe fouling, flow condition, water conductivity and water temperature. Especially, the multi-peaked output signal above the preset level, which is caused by a chaotic motion of the bubble, coalescence of bubbles or wetting of the probe tips, affects the measurement of the bubble frequency. Recently, Liu(1991) developed a new iterative algorithm. He determined the cutoff level by comparison with channel-averaged void fractions obtained by the quick closing method in the air-water flow. But it is difficult to apply this algorithm in steam-water boiling experiments as in this study. Thus, here, a new computer algorithm for the phase discrimination of steam-water boiling flow was developed. The new algorithm is also based on the pulse height and the slope criterion as previous investigators. The difference is that the cutoff level for each bubble is calculated based on the slope criterion and the pulse height for each bubble instead of the constant preset cutoff level for all bubbles. That is, the cutoff level for each bubble is proportional to the pulse height produced by individual bubbles. But the phase discrimination above the cutoff level is carried out by slope condition. The proportional constant is predetermined by air-water experiments and found to be 0.55. The main advantage of this algorithm is that the cutoff level for each bubble is varied according to the signal variations induced by factors mentioned above. The algorithm is based on the fact that the pulse heights of the output signals are different for all bubbles. If the pulse height is lower than a presetted cutoff level, the pulse will be neglected in the calculations of local parameters even though it is explicitly generated by a bubble. But the present algorithm will identify the signal as a bubble.

3.1.3 Calculations of local vapor parameters

(1) Calculation of the local void fraction and the bubble frequency

The local void fraction can be calculated from the converted two-value signal obtained by the phase discrimination scheme. It is defined as the fraction of bubble elapsed time and total measuring time at the local position. For the statistical treatment of local void fractions, the total measuring time should be sufficiently long. In this study, total measuring time for each local position is set to about 2 minutes, which is long enough to guarantee repeatable void fractions. The void fraction is determined by the upstream signal of the two-conductivity probe because the downstream signal is affected by the wake of a bubble that passed the start probe. The local bubble frequency, defined as the number of bubbles that pass through the point per unit time, is also measured at the start probe. It will be used in the evaluation of the local IAC of the two-fluid model.

(2) Calculation of the local vapor velocity and its spectrum

The local vapor velocity can be calculated based on the elapsed time at the boundaries between vapor and liquid phases, if it is assumed that all the bubbles are in uni-directional motion and a bubble hitting the start probe will sequently hit the stop probe. The local vapor velocity V_b can be calculated if the mean elapsed time τ is known as follows.

$$V_b = \Delta Z / \tau \qquad (1)$$

A bubble hitting the start probe will not always pass the stop probe. Thus, the identification of the probe signals is necessary. It is performed by comparing the chordal length of the start probe with that of the stop probe. If the chordal length of the stop probe is within $\pm 30\%$ compared to that of the stop probe, then the signal of the start probe is considered as that of the stop probe.

The local mean velocity is calculated arithmetically from the velocity spectrum. Also the velocity fluctuation, that is the turbulent fluctuation of a bubble, is obtained by calculating the standard deviation of the bubble velocity.

(3) Calculation of the local IAC and the Sauter mean diameter

A lot of works has been carried out to determine the IAC by experiments and analysis, but most of studies were limited to the measurements of the area-averaged or volume-averaged IAC in the air-water two-phase flow. Generally, they were measured by the light attenuation technique, the chemical technique and the high-speed photo graph technique. In this study, the local IAC was measured using the methodology of Kataoka et. al (1984).

They derived following Eq. (4) by assuming that the turbulent fluctuation of a bubble velocity may be approximately isotropic and the bubble shape is spherical.

$$a_i(r) = \frac{4N_t\left\{\sum_j \frac{1}{|v_{szj}|} / (\sum_j)\right\}}{1-\cot\frac{\alpha_0}{2}\ln\left(\cos\frac{\alpha_0}{2}\right)-\tan\frac{\alpha_0}{2}\ln\left(\sin\frac{\alpha_0}{2}\right)} \qquad (2)$$

where

$$\frac{\sin 2\alpha_0}{2\alpha_0} = \frac{1-(\sigma_z^2/|\overline{v_{sz}}|^2)}{1+3(\sigma_z^2/|\overline{v_{sz}}|^2)} \qquad (3)$$

$$\sigma_z = \left(\sum_j N_{szj}\cdot(v_{szj}-v_{sz})^2 / \sum_j N_{saj}\right)^{1/2} \qquad (4)$$

Using above Eqs. (2), (3) and (4), the local IAC can be calculated by measuring the local vapor velocity spectrum and bubble frequency for each measuring point. These can be applied to the forced subcooled boiling regime where small bubbles move mainly in the axial direction and the average lateral motion must be very small.

In this study, the Sauter mean diameter was calculated to analyze the IAC. The reason that the Sauter mean diameter is the most important length scale in the analysis of the IAC is the definition of the Sauter mean diameter is similar to that of the IAC. The local Sauter mean diameter can be calculated as follows by assuming that the bubble is spherical.

$$D_s = \frac{6\alpha}{a_i} \qquad (5)$$

3.1.4 Verifications of the void fraction and the vapor velocity

The local void fraction is verified by separate air-water experiments in a cylindrical glass tube of 8 mm inner diameter. Area-averaged void fractions are calculated by measuring the entrapped air volume and compared to cross-sectional integrated local void fractions measured by a two-conductivity probe. The flow conditions of the test loop are 0.5m/sec~3m/sec of liquid velocities and 1.9%~42.4% of area

-averaged void fractions. The maximum relative error and standard deviation of the area-averaged void fraction are 8.6% and 1.008%, respectively.

Verification of the vapor velocity is carried out by and analysis of high speed photograph. The high speed camera of PHOTEC whose maximum shutter speed is 10000 frames/sec is used for this analysis. The shutter speed is set to 4000 frames/sec in experiments. The maximum relative error and standard deviation of local vapor velocities are 4.52% and 3.08%, respectively.

3.2 Measurement of the local liquid velocity

In this study, the distributions of the liquid velocity in the boiling channel was measured by a Pitot tube. The problems of a Pitot tube to the application in two-phase flow is that the possibility of gas or vapor inflow into the Pitot tube is large and it may disturb the flow field. To avoid the former problem, the pressure holes of the Pitot tube and the volume exchange between the pressure tube and the sensor cell which is caused by pressure fluctuations in the two-phase stream should be small. The latter problem is minimized by adopting a small size Pitot tube. In this study, a 1/16″ Pitot tube of UNITED SENSOR is used. The dynamic pressure is measured by CD-15 demodulator and DP-103 differential pressure transducer of VALIDYNE, which is the diaphragm changeable type. These instruments minimize the possibility of the problems of vapor inflow into the pressure tube and disturbance of the flow field. But the cold water injection system is made to get rid of vapor phase entrapped in the Pitot tube. In this study, the local liquid velocity is calculated using the Bosio & Malnes model as follows;

$$v_L=\frac{1}{\sqrt{1-a^2/2}}\sqrt{\frac{2\Delta p}{k\rho_L}} \qquad (6)$$

The measurements of the momentum transfer factor k is requisite in the application of the low liquid velocity region because the drag force at the Pitot tube tip is changed rapidly according to the liquid velocity. The determination of k was carried out in the experiments of the single phase flow. The model showed good agreement with the average liquid velocities obtained by volume measurements in air-water experiments. In these tests, the maximum relative error was 4.2%.

4. Measurements

Measurements were performed with varying heat flux and flow condition. A total of 48 sets of experiments were carried out in the subcooled boiling. A summary of the experimental conditions are described in Table 1.

Table 1 Experimental conditions

Parameter	Range
Superficial liquid velocity	0.45~2m/sec
Area-averaged void fraction	0~10%
Local void fraction	0~35%
Inlet subcooling	3~45℃
Heat generaton rate	10~30 kW
System pressure	1bar(48sets)

5. Results and Discussions

Distributions of the Local Void Fraction and the Bubble Frequency

In air-water flow, the interfacial transfer terms such as the interfacial mass transfer and interfacial energy transfer, are negligible because the physical quantities such as the pressure and the temperature between phases are negligible. However, in the boiling flow, those terms can not be negligible due to phase change. Thus, the distributions of the two-phase flow parameters in air-water flow and in steam-water boiling flows will be different explicitly for these interfacial transfer phenomena. Among these parameters, the local void fraction is most important because it reflects the energy of the fluid and its distribution affects the distributions of another local parameters such as the vapor velocity, the liquid velocity and the local IAC in the two-phase flow.

In air-water experiments, the peaking of the local void fractions near the wall are reported by many investigators. It is known that the phenom-

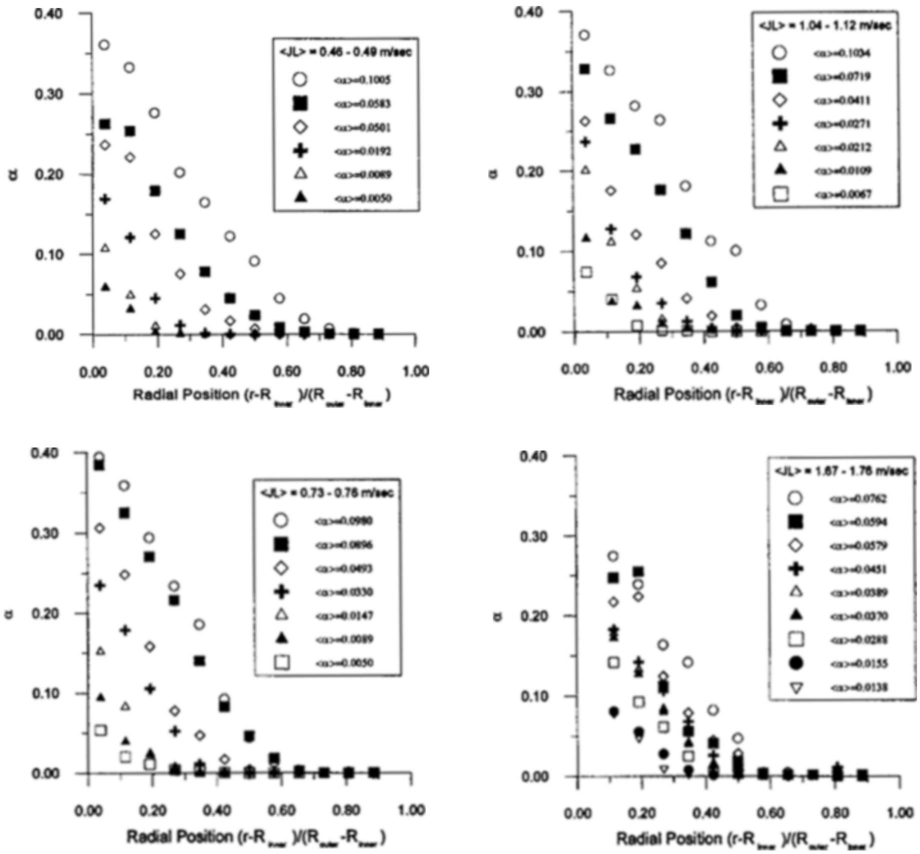

Fig. 3 Radial distributions of local void fraction in the annulus loop

ena is happened by the migration of bubbles toward the wall and then the bubble frequency profiles are similar to those of local void fractions. Up to now, the reasons of this wall peaking phenomena are known that the unbalanced lateral pressure gradient around the bubble-liquid interface resulting from the interaction with the liquid phase gradient and the vortex resulting from the deformed bubbles near the wall give the lift force to the bubbles toward the wall.

However, the wall peaking caused by the lift force was not observed in this steam-water boiling experiments. The radial profiles of the local void fractions for various flow conditions and the area-averaged void fractions are shown in Fig. 3. In the figure, $(r-R_{\mathrm{inner}})/(R_{\mathrm{outer}}-R_{\mathrm{inner}})=0$ means the surface of a heating rod and $(r-R_{\mathrm{inner}})/(R_{\mathrm{outer}}-R_{\mathrm{inner}})=1$ means the outer wall of on annulus channel. As shown in this figure, the local void fractions for all flow conditions smoothly decayed out from the surface of the heating rod to the outer wall. These distributions of the local void fraction is quite different from those of air-water experiments performed by other investigators where wall peaking were observed. The distributions coincide with those of the local internal energy in the subcooled boiling.

To obtain more informations about the internal structure of the subcooled boiling, the distributions of the bubble frequency should be known. The radial profiles of local vapor bubble frequencies are shown in Fig. 4. The profiles are similar to those of local void fractions, that is, the bubble frequency is high where the local void

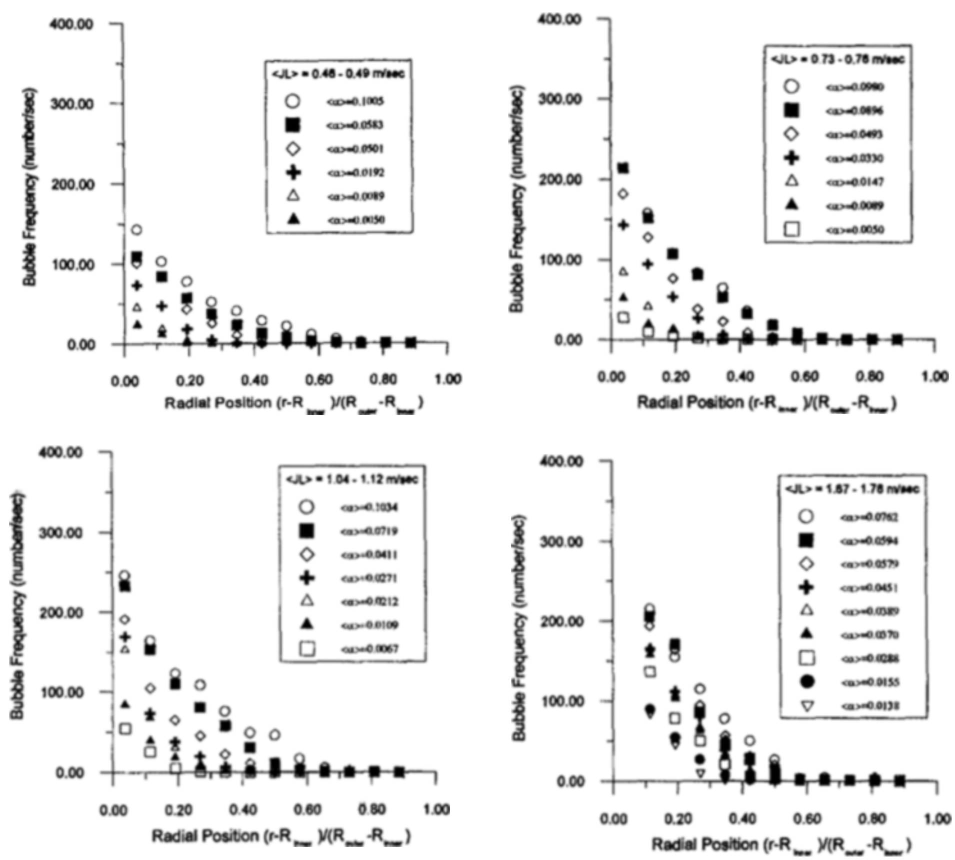

Fig. 4 Radial distributions of local bubble frequency in the annulus loop

fraction is high. It shows that the increase of local void fraction caused by increase of an internal energy is not due to the increase of a the vapor bubble size but mainly due to the increase of the vapor bubble frequency for a given area-averaged void fraction in the subcooled boiling.

Distributions of Local Phasic Velocities

The local vapor bubble velocity and liquid velocity were measured simultaneously in this study. It is known that the vapor velocity is greater than the liquid velocity in two-phase flow. It is due to the buoyancy force caused by the density difference between phases. And the slip ratio of low liquid flow condition is larger than that of high flow condition and the distributions of local phases velocities are affected by the phase distributions in the channel.

The radial profiles of local phases velocities for various flow conditions and area-averaged void fractions are shown in Figs. 5 and 6, respectively.

As shown in Fig. 5, the vapor velocities at the center of the channel are higher than those at the heating rod. But a sudden decrease of the bubble velocity near the heating rod was observed in the low flow conditions such as 0.46m/sec~0.49m/sec of $\langle j_l \rangle$, even though such a decrease of bubble velocity is not observed in the higher flow conditions. In the high void crowded region, the phase velocities are increased due to high buoyancy effect. But the sudden decrease of the vapor velocity is seemed due to the micro pumping induced phenomena. If bubbles are ejected from the boiling site, the pressure at that position is suddenly

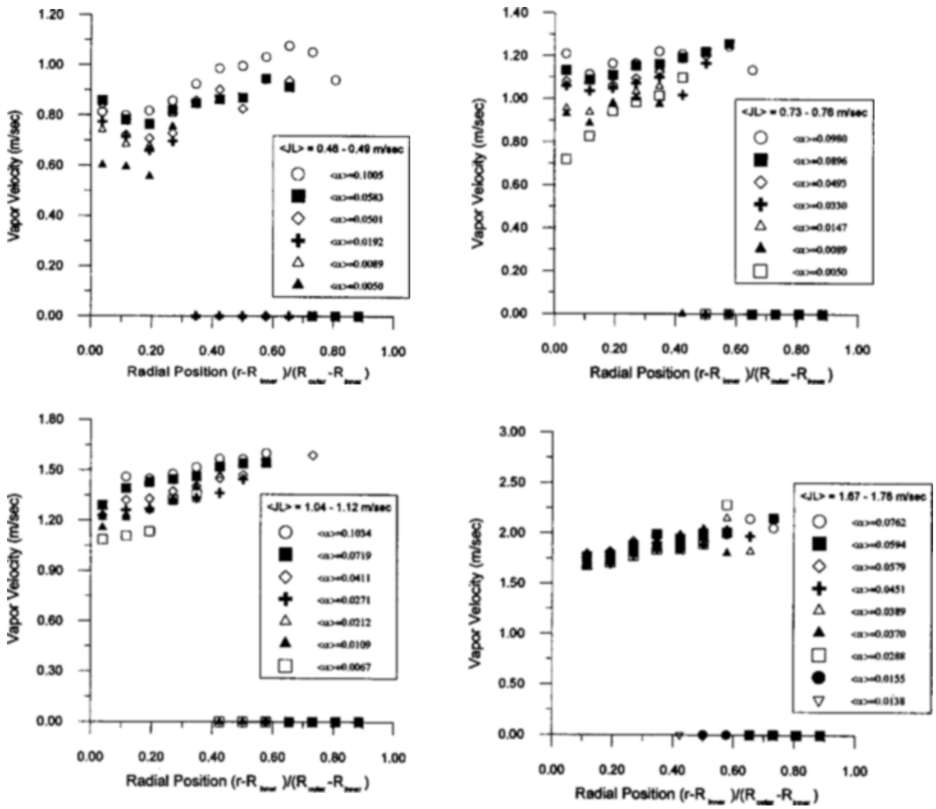

Fig. 5 Radial distributions of local vapor velocity in the annulus loop

decreased and so the liquid phase moves to the lateral direction. The lateral velocity of liquid phase is increased and then the axial liquid velocity will be decreased and also the axial bubble velocity will be decreased. The liquid velocity profiles in Fig. 6 confirm this explanation. In high flow condition, the lateral liquid velocity is relatively small compared to the axial liquid velocity and so the phenomena is suppressed by liquid inertia force. However, more investigation is needed to understand this phenomena in the annulus boiling channel.

Figure 6 shows the profiles of local liquid velocities. In the single phase flow, the velocity profile is parabolic due to the effect of shear force at the channel wall. However, in the two-phase flow, the nonuniformity of void distribution and bubble velocity across the test section change the liquid velocity profile from the shape in the single phase liquid flow. The position of the maximum velocity of the liquid phase is moved toward the heating rod as the area-averaged void fraction increases for all flow conditions. These trends imply that the high velocity phase lifts the low velocity phase.

The radial profiles of the local slip ratio are shown in Fig. 7. The profiles of the local slip ratio are similar to those of the vapor bubble velocity. The local slip ratios at the channel center are higher than those near the heating rod. The slip ratio increases as the area-averaged void fraction increases for a given liquid flow condition and decrease as the area-averaged liquid superficial velocity increases. The reason of the trend according to liquid flow condition is that the increase of the vapor bubble velocity driven by the buoyancy force is suppressed by the increase of inertia force.

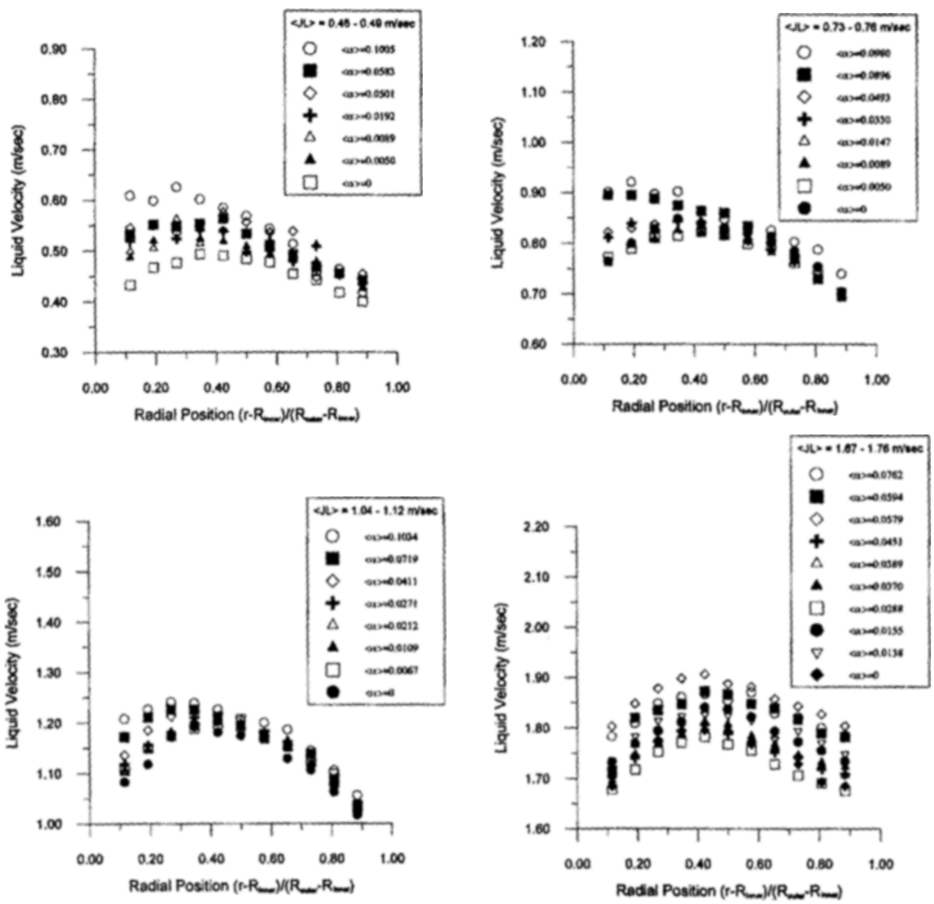

Fig. 6 Radial distributions of Local liquid velocity in the annulus loop

It is interesting that the local slip ratios around the heating rod for high flow conditions such as 1.04m/sec~1.76m/sec of $\langle j_l \rangle$ are less than 1, that is, the liquid velocity is faster than the vapor bubble velocity. The first reason is the effect of wall shear stress of liquid phase and the second is that the velocity of the vapor bubble around the heating rod is not reached terminal velocity for high flow condition.

The radial profiles of turbulent intensity of vapor bubble at various flow conditions and area-averaged void fractions are shown in Fig. 8. The profiles of relative turbulent fluctuations of vapor bubbles are decayed out from the surface of the heating rod to the channel center. The effect of ... of the area-averaged void fraction was to increase the relative velocity fluctuation of the vapor bubble for a given flow condition. But the increasing of area-averaged liquid superficial velocity decrease the relative velocity fluctuations of the vapor bubbles. The relative velocity fluctuations of vapor bubbles decrease as the average liquid velocity increase. It is due to that the relative velocity fluctuation of the vapor bubble is suppressed by increase of inertia force of liquid phase.

Distributions of the Local IAC and the Sauter Diameter

The IAC is the most important parameter in the two-fluid model. To analyze the local IAC, the bubble size should be considered simultaneously,

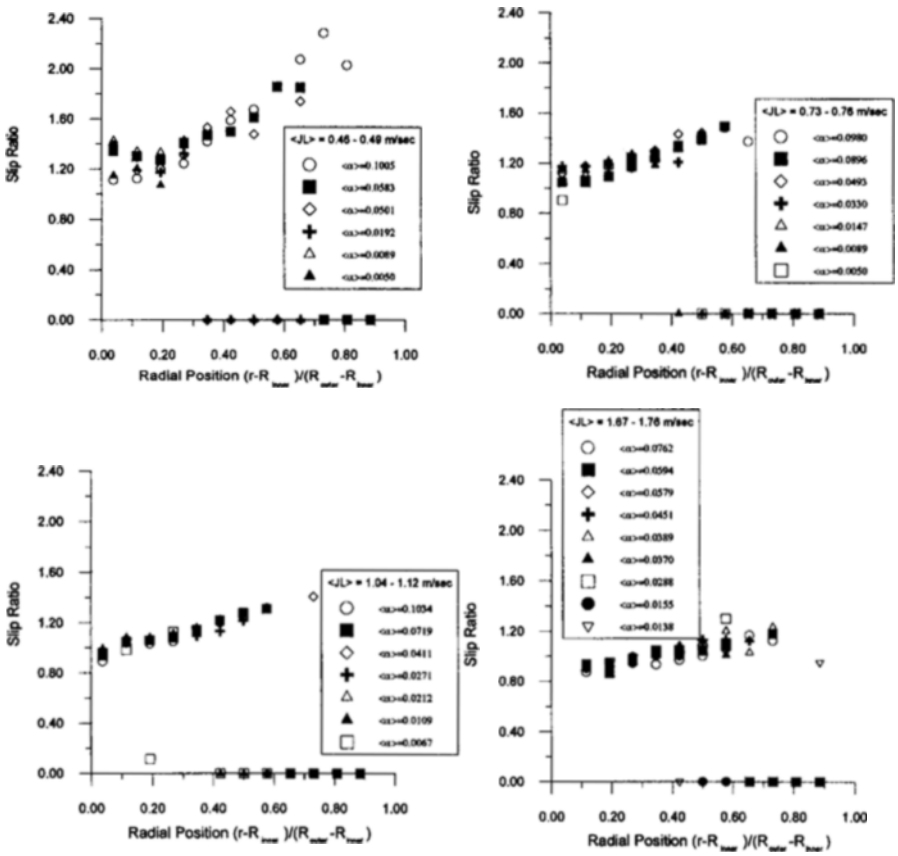

Fig. 7 Radial distributions of local slip ratio in the annulus loop

since the local void fraction is the product of the bubble number density and the volume of a bubble. The radial distributions of the local IAC and the Sauter mean diameter are shown in Figs. 9 and 10, respectively.

In Fig. 9, the radial distribution of the local IAC is similar to that of the local void fraction for a given area-averaged void fraction. This also means that bubble coalescing due to increase of the local void fraction is not significant as discussed in previous section. The evidence for this is shown explicitly by comparison of the distributions of vapor bubble frequency in Fig. 4 and the local Sauter mean diameter in Fig. 9, simultaneously. In Fig. 4, the bubble frequency distributions are similar to those of the local void fractions which are same as the local IAC distributions. In addition, the variations of order of the Sauter mean diameter are smaller than those of the vapor bubble frequency for a given area-averaged void fraction.

These results imply explicitly that the most dominant cause of increase of local IAC due to increase of the local void fraction is resulted from the increase of bubble frequency for the same area-averaged void fraction in the steam-water boiling flow. This is the same result with air-water experiment of earlier researchers such as Serizawa and Kataoka (1990). They studied the bubble size effect on the local IAC using the bubble size controlling technique at the channel entrance in their air-water experiments. They reported that the bubble frequency and the bubble size are determined by air nozzle type of the bubble

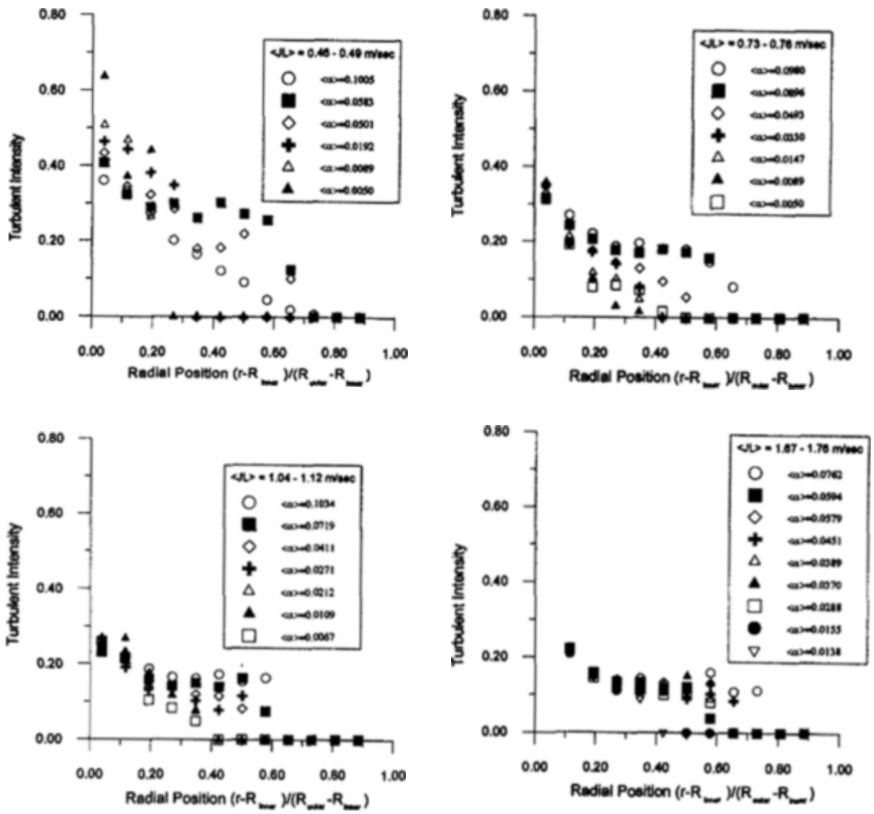

Fig. 8 Radial distributions of local bubble turbulent fluctuation in the annulus loop

generation system and so the local IAC also depends on the bubble size and the bubble frequency at the channel entrance. However, in the steam-water boiling flow, the bubble frequency and the bubble size are determined by enthalpy distribution, instability of bubble motion and fluid properties in the test channel. As shown in Fig. 10, the local Sauter diameter depends not on the area-averaged liquid superficial velocity but mostly on the area-averaged void fraction as in the case of the local IAC. It implies that the local Sauter diameters can be assumed to be constant for a given area-averaged void fraction.

6. Summary and Conclusion

The two-conductivity probe and Pitot tube methods are applied to the steam-water flow boiling in an annulus-type channel to measure the local flow parameters such as phasic velocity, IAC and void fraction. Major findings in this study can be summarized as follows:

(1) In the two-conductivity probe method for the local measurements of vapor phase, a new cutoff algorithm was successfully developed for the phase discrimination of steam-water boiling flow. And in the Pitot tube method, for boiling two-phase flow condition, the local liquid velocities were calculated successfully by modifying the Bosio & Malnes model.

(2) The void fraction distribution decays out from the surface of the heating rod to the outer wall in subcooled boiling without any wall peaking, which were observed in air-water experiments. And the increase of the local void fraction is mainly due to the increase of the vapor bubble frequency for a given area-averaged void fraction in the subcooled boiling.

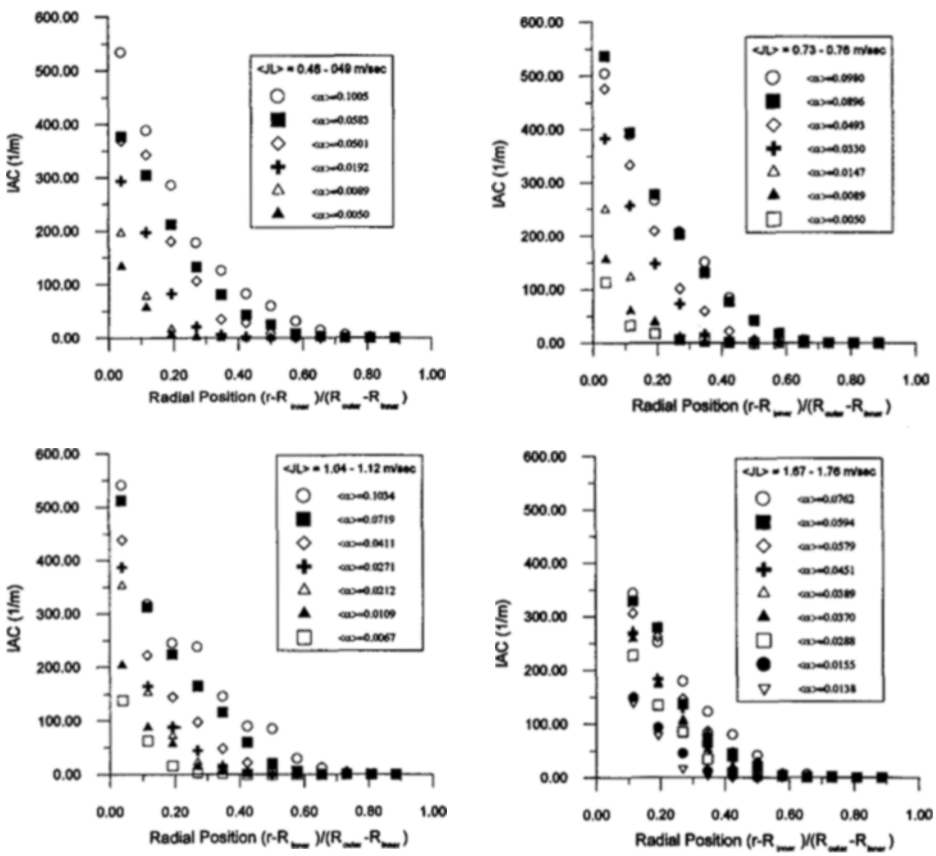

Fig. 9 Radial distributions of local interfacial area concentration in the annulus loop

(3) Vapor velocities at the channel center are higher than those near the channel wall region. But sudden decreases of the vapor velocity around the heating rod are observed in low flow conditions. And the profiles of liquid velocity are parabolic and the maximum velocity of liquid phase moves toward the heating rod as the average void fraction increases in the annulus channel. The profiles of local slip ratio are similar to those of the vapor bubble velocity.

(4) The profiles of relative turbulent fluctuations of vapor bubbles are decayed out from the heating rod to the channel center.

(5) The distributions of the local IAC are similar to those of the local void fraction for a given area-averaged void fraction.

References

Banerjee. S. and Nguyen. D. M., 1977 "Mass Velocity Measurement in Steam-Water Flow by Pitot Tubes," *AIChE Journal* Vol. 23, No. 3, pp. 385∼387.

Delhaye. J. M. and Cognet. G., 1984, *Measuring Techniques in Gas-Liquid Two-Phase Flows*, Springer-Verlag.

Fincke. J. R. and Deason. V. A., 1979, "The *Measurement of Phase Velocities in Mist Flows Using Stagnation Probes*," NUREG/CR-0648.

Herringe. R. A. and Davis. M. R., 1976, "Structural Development of Gas-Liquid Mixture Flows," *J. Fluid Mech.* Vol. 73, part 1, pp. 97∼123.

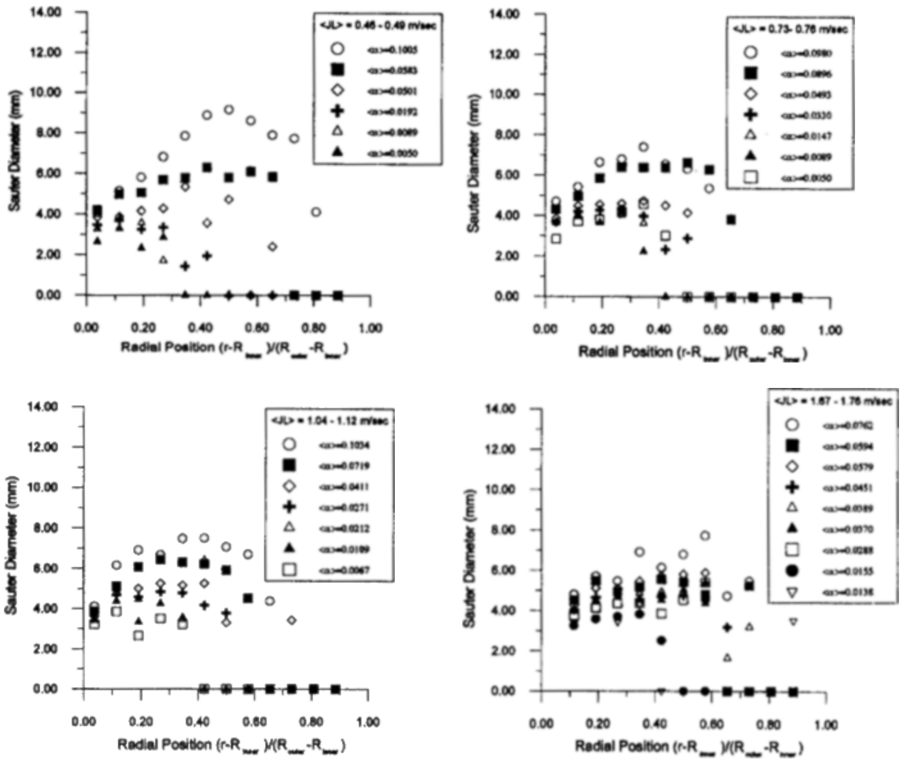

Fig. 10 Radial distributions of local sauter diameter in the annulus loop

Herringe. R. A. and Davis. M. R., 1978, "Flow Structure and Distribution Effects in Gas-Liquid Mixture Flows," *Int. J. Multiphase Flow*, Vol. 4, pp. 461～486.

Hewitt. G. F., 1978, *Measurement of Two -Phase Flow Parameters*," Academic Press.

Ishii. M. and Mishima. K., 1980, "Study of Two -Fluid Model and Interfacial Area," NUREG/ CR-1873.

Ishii. M. and Revankar. S. T., 1990, "*Local Interfacial Area Concentration Measurements* in *Bubbly Flow*," ANL-90/51.

Kataoka. I., Ishii. M. and Serizawa. A., 1984, "*Local Formulation of Interfacial Area Concentration and Its Measurements in Two-Phase Flow*," NUREG/CR-4029.

Kataoka. I. and Serizawa. A., 1990," Interfacial Area Concentration in Bubbly Flow," *Nuclear Engineering and Design*, Vol. 120, pp. 163～180.

Kataoka. I., Ishii. M. and Serizawa. A., 1994, "Sensitivity Analysisof Bubble and Probe Geometry on the Measurements of Interfacial Area Concentration Gas-Liquid Two-Phase Flow," *Nuclear Engineering and Design*, Vol. 146, pp. 53～69.

Lamb. D. E., Manning. F. S. and Wilhelm. R. H., 1960, "Measurement of Concentration Fluctuations with an Electrical Conductivity Probe," *A. I. Ch. E. Journal*.

Liu. T. J., 1989, *Experimental Investigation of Turbulence Structure in Two-Phase Bubbly Flow*, Ph. D. Thesis of Northwestern University.

Nasso. G. P., 1963, "*Development of an Electrical Resistivity Probe for Void Fraction Measurements in Air-Water Flow*," ANL-6738.

Neal. L. G. and Bankoff. S. G., 1963, "A High Resolution Resistivity Probe for Determination of Local Void Properties in Gas-Liquid Flow," *A. I. Ch. E. Journal*, pp. 490～494.

Neal. L. G. and Bankoff. S. G., 1965, "Local

Parameters in Cocurrent Mercury-Nitrogen Flow," *A. I. Ch. E Journal*, pp. 624~635.

Reimann. J., Kusterer. H. and John. H., 1983, "Two-Phase Mass Flow Rate Measurements with Pitot Tubes and Density Measurements," *Measuring Techniques in Gas-Liquid Two-Phase Flows, Symposium*, Nancy, France july 5~8.

Sekoguchi. H. F., Matsuoka. T. and Nishikawa. K., 1974, "Studies on Statistical Characteristics of Bubbles by Electrical Resistivity Probe, I, II," *Trans. JSME*, Vol. 40, p. 2295.

Serizawa. A. et al, 1974, "Turbulence Structures of Air-Water Bubbly Flow," *Int. J. Multi Phase Flow*, Vol. 2, pp. 221~233.

Sim. S. K. and Lahey. R. T. Jr., 1986, "Measurement of Phase Distribution in a Triangular Conduit," *Int. J. Multiphase Flow* Vol. 12, No. 3 pp. 405~425.

Walmet, G. E. and Staub. F. W., 1969, "Pressure, Temperature and Void Fraction Measurement in Nonequilibrium Two-Phase Flow," *Two-Phase Flow Instrumentation*, pp. 89~101.

Welle. R. V., 1985, "Void Fraction, Bubble Velocity and Bubble Size in Two Phase Flow," *Int. J. Multiphase Flow*, Vol. 11, pp. 317~345.

Yun, B. J. 1996, *Measurements of Two-Phase Flow Parameters in the Subcooled Boiling*, Ph. D thesis. Seoul National University in Korea.